

Handout 21: Stellar differential rotation

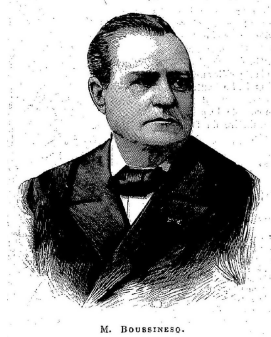


Figure 1: Joseph V. Boussinesq (1842–1929)

The first turbulence model goes back to Boussinesq (1877) and assumes that the momentum transfer caused by turbulent eddies can be modeled with an eddy viscosity, in analogy with the momentum transfer caused by the molecular motion in a gas that can be described by a molecular viscosity.¹ The Reynolds² stress is then given by (see pp. 176–180 Davidson, 2015)

$$\overline{u_i u_j} = -\nu_t (\overline{U_{i,j}} + \overline{U_{i,j}}). \quad (1)$$

At the time, this was just a postulate, but it can also be computed rigorously under the assumption that the turbulent eddies are small compared with the typical scales of the mean flow and that the Reynolds number is small. Analogously to the turbulent magnetic diffusivity, the value of ν_t is proportional to $\tau \overline{u^2}$, but with a prefactor that is usually not $1/3$, but between $2/15$ (for small Reynolds numbers) and $4/15$ (for large Reynolds numbers).

Alternatively, one can use Equation (1) to “measure” ν_t by measuring $\overline{u_i u_j}$ in a given shear flow. This works well for imposed shear flows such as the flows modeled in the shearing box approximation, but it fails when applied to the solar differential rotation, where we one can measure the correlation between u_θ and u_ϕ . This was first done by Ward (1965) for sunspot *groups* and later by Gilman & Howard (1984) for individual sunspots. Nowadays, we can use Dopplergrams from the Helioseismic and Magnetic Imager (HMI) on board the *Solar Dynamics Observatory (SDO)*. Such a result is shown in Figure 2.

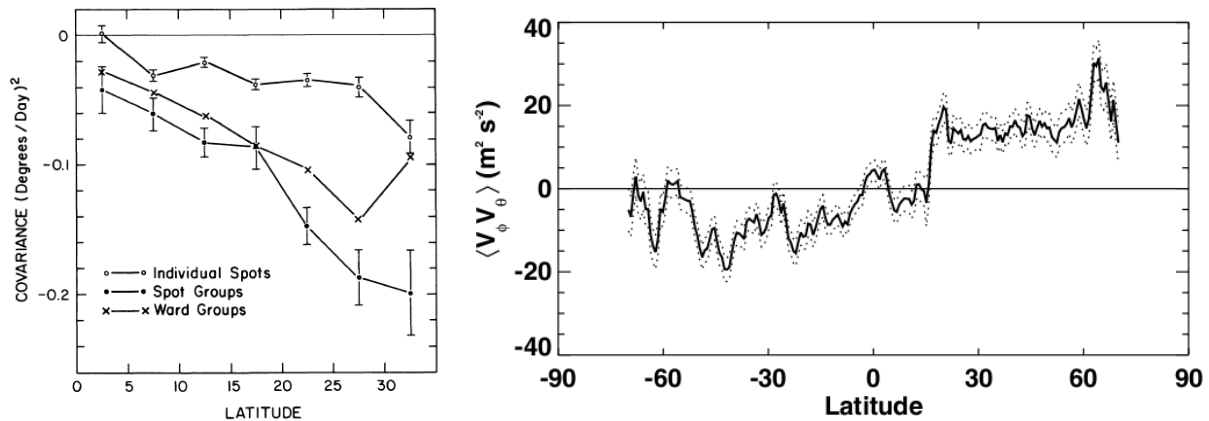


Figure 2: *Left:* Figure from Gilman & Howard (1984) showing the correlation between longitudinal and latitudinal sunspot *proper motions* versus latitude. They analyzed the Greenwich data record, covering 62 years. *Right:* Figure from Hathaway et al. (2013) showing $\overline{u_\theta u_\phi}$ versus latitude using HMI data Dopplergrams.

In meteorology, one usually works with latitude rather than colatitude. This is also what Gilman & Howard (1984) did, which explains the different signs in Figure 2. So, $\overline{u_\theta u_\phi} > 0$ in the north and negative in the south. Let us compare this with the Boussinesq ansatz (as it is usually called). Applied to spherical geometry, assuming axisymmetry for the mean flow, we have

$$\overline{u_\theta u_\phi} = -\nu_t \sin \theta \frac{\partial \overline{\Omega}}{\partial \theta}. \quad (2)$$

¹http://www.cfd-online.com/Wiki/Boussinesq_eddy_viscosity_assumption

²Osborne Reynolds FRS (1842–1912) was born in the same year as Boussinesq. He came up with the Reynolds decomposition, $\mathbf{U} = \overline{\mathbf{U}} + \mathbf{u}$, and the Reynolds rules, all of which are important for developing a theory for the Reynolds stress tensor.

Here, $\bar{\Omega} = \bar{U}_\phi / r \sin \theta$ is just a shorthand for the longitudinal mean velocity in a *non-rotating* frame of reference. This $\bar{\Omega}$ is therefore not to be confused with the vector $\mathbf{\Omega}$ is a nonrotating frame of reference, in which $\mathbf{\Omega}$ leads to a Coriolis force, for example, but not so $\bar{\Omega}$.

Let us now think about the signs. $\overline{u_\theta u_\phi}$ is measured too be positive in the north, but in the north, Ω increases with increasing θ , i.e., as we go from the pole toward the equator. Thus, $\partial \bar{\Omega} / \partial \theta$ is positive, and so is $\sin \theta$, so the signs do not match. This was recognized early on, as is evidenced by a statement from Ward (1965); see Figure 3.

Furthermore, this mean ‘‘equatorial acceleration’’ is *maintained against as-yet unspecified dissipative forces by the transport of angular momentum from regions in middle or high latitudes by selective horizontal eddy processes.* Since there is no way at present of estimat-

Figure 3: Statement from Ward (1965). He goes on to say that if this source of momentum were shut off, this layer of the Sun would reach solid rotation in about 103 days.

1 Computing the Reynolds stress

We show here two different calculations. We begin with a local and simplistic calculation (neglecting the pressure and nonlinear terms) in a rotating frame of reference using the Coriolis force in Cartesian coordinates, so the partial time derivative of the velocity fluctuation is

$$\dot{u}_i = \dots - 2\epsilon_{ikl}\Omega_k u_l + \dots \quad (3)$$

To compute the time derivative of the Reynolds stress $Q_{ij} \equiv \overline{u_i u_j}$, let us also write

$$\dot{u}_j = \dots - 2\epsilon_{jkl}\Omega_k u_l + \dots \quad (4)$$

so that $\dot{Q}_{ij} = \overline{\dot{u}_i u_j} + \overline{u_i \dot{u}_j}$ is given by

$$\dot{Q}_{ij} = \dots - 2\epsilon_{ikl}\Omega_k \overline{u_j u_l} - 2\epsilon_{jkl}\Omega_k \overline{u_i u_l} + \text{diffusive terms.} \quad (5)$$

Thus, for example,

$$\dot{Q}_{xy} = \dots - 2\epsilon_{xkl}\Omega_k \overline{u_y u_l} - 2\epsilon_{ykl}\Omega_k \overline{u_x u_l} + \dots \quad (6)$$

There will be only 2 terms from each of the ϵ terms, i.e. ϵ_{xyz} and ϵ_{xzy} as well as ϵ_{yzx} and ϵ_{yxz} . Thus, we have

$$\dot{Q}_{xy} = \dots - 2\epsilon_{xyz}\Omega_z \overline{u_y u_x} - 2\epsilon_{xzy}\Omega_z \overline{u_y u_x} - 2\epsilon_{yzx}\Omega_x \overline{u_x u_x} - 2\epsilon_{yxz}\Omega_x \overline{u_x u_x} + \dots \quad (7)$$

Thinking ‘‘perturbatively’’, where we want to explain off-diagonal terms of Q_{ij} being produced by turbulence in the presence of rotation, we can neglect off-diagonal terms on the rhs of Equation (7). Using also $\epsilon_{xzy} = -1$ and $\epsilon_{yzx} = 1$, we have

$$\dot{Q}_{xy} = \dots - 2\epsilon_{xzy}\Omega_z \overline{u_y u_x} - 2\epsilon_{yzx}\Omega_x \overline{u_x u_x} + \dots = \dots + 2\Omega_z \left(\overline{u_y^2} - \overline{u_x^2} \right) + \dots \quad (8)$$

So, in a rotating system, *off-diagonal terms are being produced if the turbulence is anisotropic* and thus $\overline{u_y^2} - \overline{u_x^2} \neq 0$.

Let us apply this now to spherical geometry by making the identification

$$(x, y, z) \rightarrow (\theta, \phi, r). \quad (9)$$

In that case we have

$$\dot{Q}_{\theta\phi} = \dots + 2\Omega_r \left(\overline{u_\phi^2} - \overline{u_\theta^2} \right) + \dots \quad (10)$$

Thus, in the north where $\Omega_r > 0$, and if the turbulent fluctuations in the longitudinal direction are stronger than the latitudinal one (which is often found to be the case in rotating systems), we expect a positive contribution to $\dot{Q}_{\theta\phi}$. It is this terms which drives latitudinal differential rotation and balances

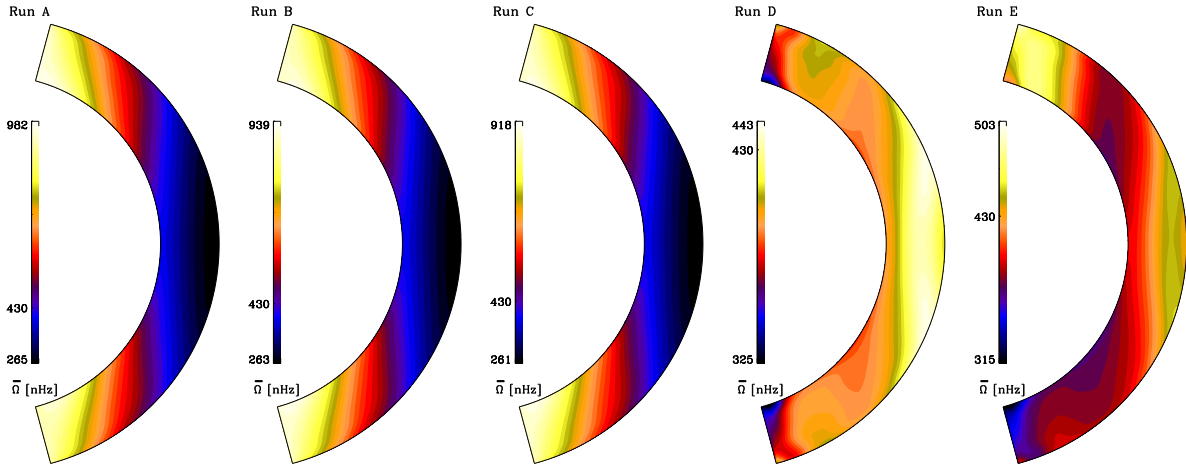


Figure 4: Time-averaged rotation profiles from Runs A–E showing $\bar{\Omega}$ in nHz. Adapted from Käpylä et al. (2014)

the diffusive term, $\nu_t \sin \theta \partial \bar{\Omega} / \partial \theta$, which must therefore also be positive. In the south, $\Omega_r < 0$, and in general we have $\Omega_r = \Omega \cos \theta$, so

$$\dot{Q}_{\theta\phi} = \dots + 2\Omega \cos \theta \left(\overline{u_\phi^2} - \overline{u_\theta^2} \right) + \dots \quad (11)$$

Similar arguments also apply to *radial differential rotation*. Making this time the identification

$$(x, y, z) \rightarrow (r, \phi, -\theta). \quad (12)$$

we have

$$\dot{Q}_{r\phi} = \dots + 2\Omega_\theta \left(\overline{u_\phi^2} - \overline{u_r^2} \right). \quad (13)$$

Here, $\Omega_\theta = \Omega \sin \theta$ is positive in both hemispheres.

We have seen that the Λ effect is related to anisotropy parameters, defined as

$$A_M = \frac{\overline{u_\theta'^2} - \overline{u_r'^2}}{\overline{u_\theta'^2} + \overline{u_r'^2}}, \quad (14)$$

$$A_V = \frac{\overline{u_\phi'^2} - \overline{u_r'^2}}{\overline{u_\phi'^2} + \overline{u_r'^2}}, \quad (15)$$

$$A_H = \frac{\overline{u_\phi'^2} - \overline{u_\theta'^2}}{\overline{u_\phi'^2} + \overline{u_\theta'^2}}. \quad (16)$$

These are shown in some of the plots in the following section.

2 Solar versus anti-solar rotation

Work over the last 5–8 years has established that the Sun should show anti-solar rotation, if all input parameters are taken at face value.

3 Another derivation

We reproduce here the derivation of Warnecke et al. (2016) and denote partial time derivatives by a dot and compute

$$\dot{Q}_{ij} = \overline{\dot{u}_i' u_j'} + \overline{u_i' \dot{u}_j'} \quad (17)$$

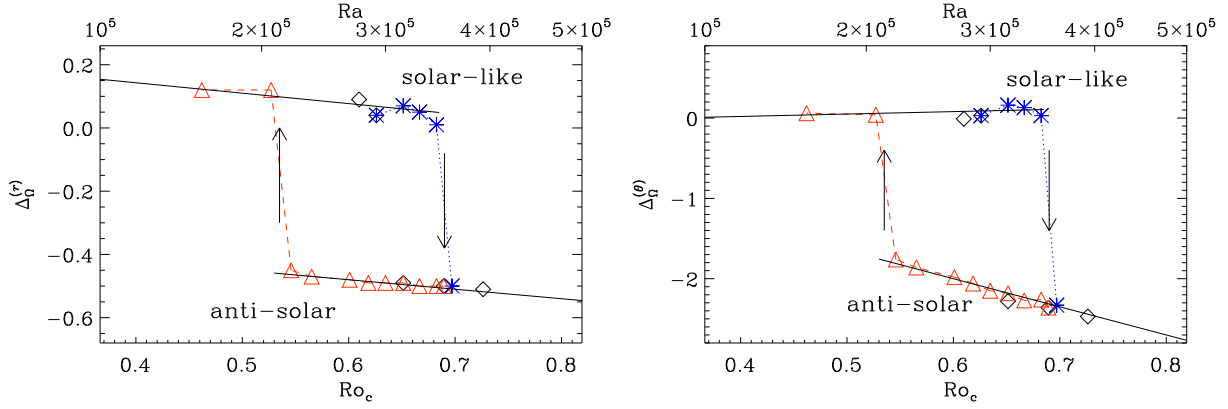


Figure 5: Radial (left panel) and latitudinal (right panel) differential rotation from Runs A–E (diamonds), and Set D (blue dotted line with asterisks) and B (red dashed line with triangles). Adapted from Käpylä et al. (2014)

in a non-rotating frame of reference ($\bar{\mathbf{U}} = \bar{\mathbf{u}} + \hat{\mathbf{e}}_\phi \Omega_0 r \sin \theta$), using

$$\dot{u}'_r = 2(u'_\theta \bar{U}_\theta + u'_\phi \bar{U}_\phi)/r + \dots, \quad (18)$$

$$\dot{u}'_\theta = -(u'_r \bar{U}_\theta + \bar{U}_r u'_\theta)/r + 2u'_\phi \bar{U}_\phi \cot \theta / r + \dots, \quad (19)$$

$$\dot{u}'_\phi = -2(u'_r \bar{U}_\phi + \bar{U}_r u'_\phi)/r - 2(u'_\theta \bar{U}_\phi + \bar{U}_\theta u'_\phi) \cot \theta / r + \dots, \quad (20)$$

where the three dots denote nonlinear and gradient terms of u_r , u_θ , and $u_\phi/r \sin \theta$ that will be neglected. Below we also consider the case where gradient terms of u_θ will be included. In other words, the base state corresponds to rigid rotation with a meridional flow $u_\theta \propto r \sin \theta$, and gradients around this state are neglected.

Inserting Equations (18)–(20) into Equation (17), we obtain an expression of the form

$$\dot{Q}_{ij} = L_{ijk} \bar{U}_k + R_{ij}, \quad (21)$$

where L_{ijk} is a rank 3 tensor (related to the coefficients of the Λ effect) and R_{ij} stands for all remaining terms, in particular those that stem from the triple correlations. In the minimal tau approximation we replace those by a relaxation term with the turbulent correlation time τ , that is $R_{ij} = -Q_{ij}/\tau$. Inserting this into Equation (21) and assuming a steady state, that is $\dot{Q}_{ij} = 0$, using that the background velocity correlation is of the form $\overline{u'_i u'_j} = \text{diag}(\overline{u'^2_r}, \overline{u'^2_\theta}, \overline{u'^2_\phi})$, we have

$$Q_{r\theta} = 2\tau(\overline{u'^2_\theta} - \overline{u'^2_r}) \bar{U}_\theta / r + \dots, \quad (22)$$

$$Q_{r\phi} = 2\tau(\overline{u'^2_\phi} - \overline{u'^2_r}) \Omega \sin \theta + \dots, \quad (23)$$

$$Q_{\theta\phi} = 2\tau(\overline{u'^2_\phi} - \overline{u'^2_\theta}) \Omega \cos \theta + \dots, \quad (24)$$

where \bar{U}_ϕ has been replaced by $\Omega r \sin \theta$ and gradient terms of u_θ/r are assumed to vanish, so that Equation (19) yields $\dot{u}'_\theta = -2(u'_r \bar{U}_\theta + \bar{U}_r u'_\theta)/r + \dots$. We note that, while $Q_{r\phi}$ and $Q_{\theta\phi}$ are proportional to Ω , the meridional component $Q_{r\theta}$ is proportional to \bar{U}_θ ($\equiv \bar{u}_\theta$). If we were to allow u_θ/r to have non-vanishing gradients, we would have $Q_{r\theta} = \tau(2\overline{u'^2_\theta} - \overline{u'^2_r}) \bar{U}_\theta / r + \dots$. In that case, under isotropic conditions ($\overline{u'^2_r} = \overline{u'^2_\theta} = \overline{u'^2_\phi}$), $\Lambda_V = \Lambda_H = 0$, but Λ_M is non-vanishing and would be positive. Therefore, the non-diffusive contribution to $Q_{r\theta}$ would be negative for a poleward flow. This is in agreement with the profiles of Λ_M and $Q_{r\theta}$ in the surface regions of our simulations.

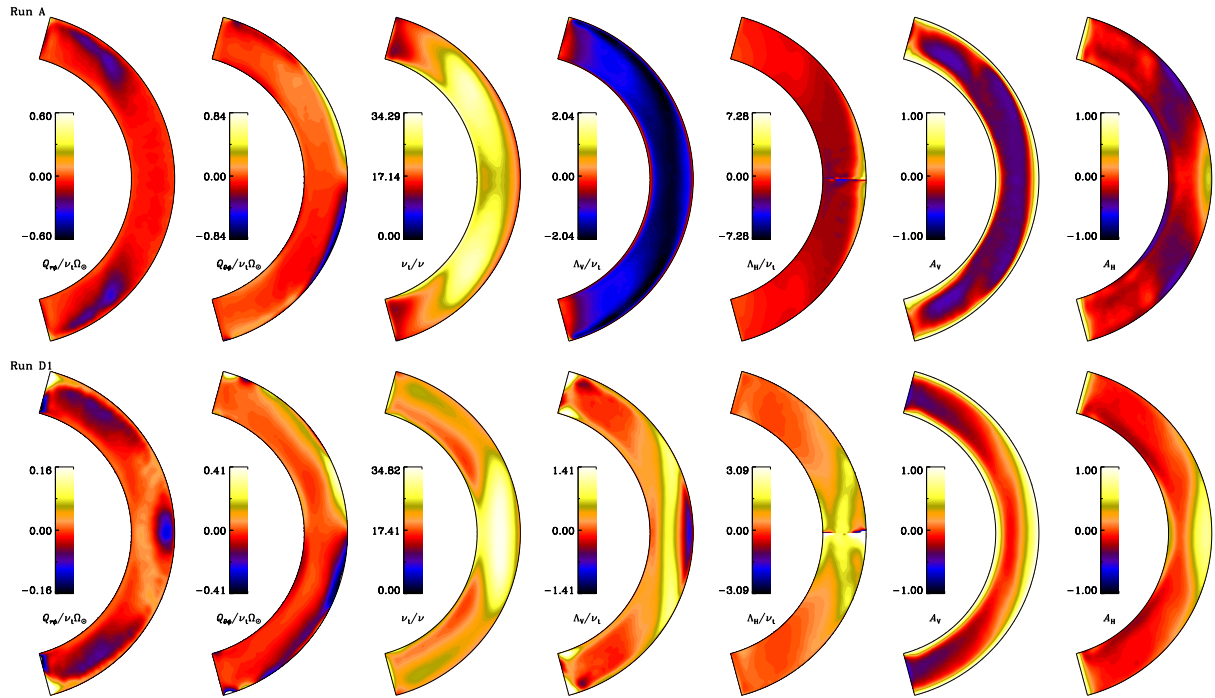


Figure 6: From left to right: Time-averaged Reynolds stresses $Q_{r\phi}$ and $Q_{\theta\phi}$ normalized by $\nu_t\Omega_\odot$, the turbulent viscosity divided by the molecular viscosity ν_t/ν , Λ_V and Λ_H normalized by ν_t , and the anisotropy parameters A_V and A_H . Top row: Run A; bottom row: Run D1. In the fifth column we only use data some degrees away from the equator so as to avoid the singularity associated with the division by $\cos\theta$. The contours in the lower row are oversaturated near the θ -boundaries in order to highlight the features at lower latitudes. Adapted from Käpylä et al. (2014)

4 Reynolds stress in the supergranulation layer

Using local helioseismology, Langfellner et al. (2015) measured the $\overline{u_\theta u_\phi}$ correlation and found the opposite sign and a ten times larger value; see Figure 7. This makes sense, because previous measurements are concerned with large length scales and reflect the flows at larger depths, while Langfellner’s values apply to the supergranulation layer, the top 3 per cent of the Sun. Here, the horizontal flow correlation comes as a consequence of the Sun’s differential rotation and is consistent with a turbulent diffusive response, while in deeper layers, anti-diffusive effects prevail.

References

- Boussinesq, J., “Essai sur la théorie des eaux courantes,” *Mémoires présentés par divers savants à l’Académie des Sciences* **23**, 1-680 (1877).
- Davidson, P. A. *Turbulence: an introduction for scientists and engineers*. Oxford: Oxford University Press (2015).
- Gilman, P. A., Howard, R., “On the correlation of longitudinal and latitudinal motions of sunspots,” *Solar Phys.* **93**, 171-175 (1984).
- Hathaway, D. H., Upton, L., & Colegrove, O., “Giant convection cells found on the Sun,” *Science* **342**, 1217-1219 (2013).
- Käpylä, P. J., Käpylä, M. J., & Brandenburg, A., “Confirmation of bistable stellar differential rotation profiles,” *Astron. Astrophys.* **570**, A43 (2014).
- Langfellner, J., Gizon, L., & Birch, A. C., “Spatially resolved vertical vorticity in solar supergranulation using helioseismology and local correlation tracking,” *Astron. Astrophys.* **581**, A67 (2015).

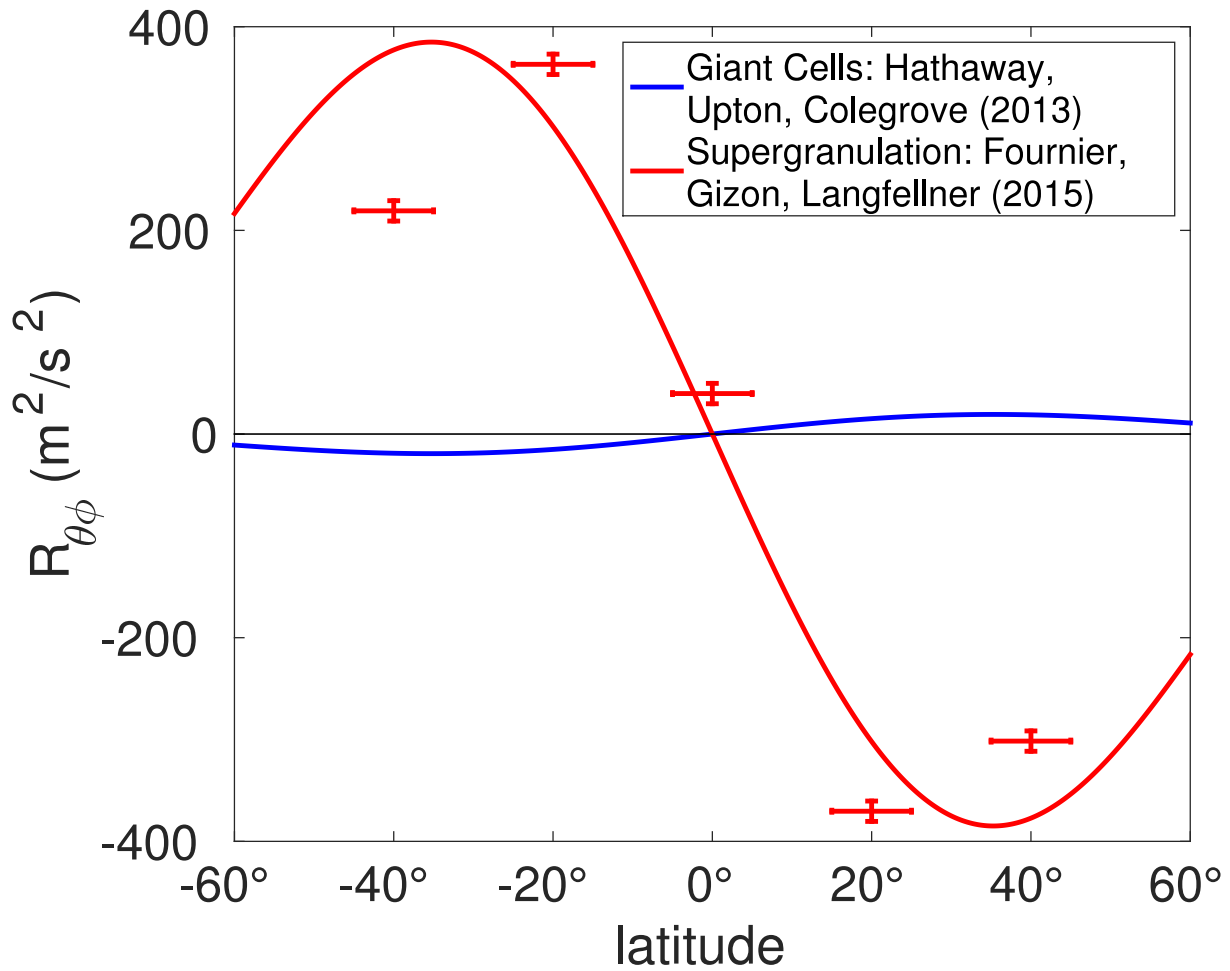


Figure 7: Comparison of $\overline{u_\theta u_\phi}$ obtained from local helioseismology (red; see Langfellner et al., 2015) and Doppler measurements (blue; see Hathaway et al., 2013).

Ward, F., “The general circulation of the solar atmosphere and the maintenance of the equatorial acceleration,” *Astrophys. J.* **141**, 534-547 (1965).

Warnecke, J., Käpylä, P. J., Käpylä, M. J., & Brandenburg, A., “Influence of a coronal envelope as a free boundary to global convective dynamo simulations,” *Astron. Astrophys.*, in press, DOI:10.1051/0004-6361/201526131 (2016).